Ocean Systems Engineering, *Vol. 6, No. 4 (2016) 325-344*
DOI: http://dx.doi.org/10.12989/ose.2016.6.4.325

CFD prediction of vortex induced vibrations and fatigue assessment for deepwater marine risers

Chetna Kamble*[1] and Hamn-Ching Chen[2]

[1]*Department of Ocean Engineering, Texas A&M University, USA*
[2]*Department of Civil Engineering, Texas A&M University, USA*

(Received July 27, 2016, Revised October 8, 2016, Accepted October 12, 2016)

Abstract. Using 3D computational fluid dynamics techniques in recent years have shed significant light on the Vortex Induced Vibrations (VIV) encountered by deep-water marine risers. The fatigue damage accumulated due to these vibrations has posed a great concern to the offshore industry. This paper aims to present an algorithm to predict the crossflow and inline fatigue damage for very long ($L/D > 10^3$) marine risers using a Finite-Analytical Navier-Stokes (FANS) technique coupled with a tensioned beam motion solver and rainflow counting fatigue module. Large Eddy Simulation (LES) method has been used to simulate the turbulence in the flow. An overset grid system is employed to mesh the riser geometry and the wake field around the riser. Risers from NDP (2003) and Miami (2006) experiments are used for simulation with uniform, linearly sheared and non-uniform (non-linearly sheared) current profiles. The simulation results including inline and crossflow motion, modal decomposition, spectral densities and fatigue damage rate are compared to the experimental data and useful conclusions are drawn.

Keywords: computational fluid dynamics; vortex-induced vibration (VIV); crossflow; inline; fatigue; riser

1. Introduction

Fatigue damage arising from Vortex-induced Vibrations (VIV) on marine risers has been a critical area of research in offshore industry in recent years. Application of concepts in VIV developed by Blevins (1990), Bearman (1984), etc., to flexible structures has been achieved by both numerical and experimental analysis. Model testing of the marine risers as well as full scale experiments have been conducted and are published by Trim, Braaten *et al*. (2005), Lie and Kassen (2006) and Tognarelli, Taggart and Campbell (2008). The search for oil and gas in deeper waters and usage of very long marine risers have posed severe challenges to the model testing facilities. The in-situ experiments are also limited by the difficulty and higher costs associated with sensor installation on the risers.

Due to increasing computational capability, numerical methods provide attractive alternative to accurately predict the complex nature of the VIV on slender bodies. Newman and Karniadakis (1997) and Meneghini, Saltara *et al*. (2004) have used numerical methods to successfully explain the dynamics of flexible bodies in different velocity profiles. These studies used a 2D simulation

*Corresponding author, E-mail: chetna_2491@tamu.edu

http://www.techno-press.org/?journal=ose&subpage=7 ISSN: 2093-6702 (Print), 2093-677X (Online)

of VIV around the marine risers. Computational fluid dynamics offers an efficient 3D simulation of flow field around the riser thereby capturing the complexities associated with these vibrations as seen in Holmes, Oakley and Constantinides (2006).

A 3D riser VIV analysis methodology has been developed by Pontaza, Chen *et al*. (2004, 2005a, b), Pontaza, Chen *et al*. (2005) and Pontaza and Chen (2007). This method uses a Finite-Analytic Navier Stokes (FANS) algorithm to simulate the flow field around the riser. An overset (chimera) domain decomposition method is employed to discretize the flow field and the riser. The riser structure is modeled as a tensioned beam and fully implicit finite difference scheme based on beam equation has been applied as developed in Huang, Chen *et al*. (2007, 2008, 2010, 2011, 2012). This time domain method is shown to be unconditionally stable in Huang, Chen *et al*. (2011).

Fatigue damage associated with VIV has been studied in detail by experimental analysis and empirical models. Norwegian Deepwater Program (NDP) conducted a series of tests on long marine riser of L/D ~ 1400 for uniform and sheared current velocities and for both bare and strake riser geometries. The experimental data was analyzed and published in Trim, Braaten *et al*. (2005) which presented both crossflow and inline fatigue and successfully tested the efficiency of the strake geometries in reducing the VIV fatigue damage. Mukundan, Modarres-Sadeghi *et al*. (2009) also used the NDP experimental data and employed a response reconstruction method to obtain the motion and strain time series from the sensors and estimated the fatigue damage from rainflow counting and Van Der Pol wake oscillator model. A semi empirical time domain simulation was conducted by Thorsen, Saevik *et al*. (2015) to quantify fatigue damage resulting from VIV. Fluid and the structure were represented by a hydrodynamic force model and Euler-Bernoulli beam equation model respectively. Another field experiment was conducted by DeepStar in Gulf of Mexico near the coast of Miami in 2006 (Vandiver, Jaiswal *et al*. 2006). This experiment simulated VIV of bare and strake riser geometries with L/D ~ 4200 to achieve higher mode responses in a non-uniform flow. Vandiver, Jaiswal *et al*. (2006) and, Jhingran and Vandiver (2007) published a fatigue analysis of the experiments associated with higher harmonics. These experiments have also been used by Constantinides and Oakley (2008) to estimate fatigue damage using a 3D CFD approach and estimated fatigue damage occurring from higher harmonics and established the presence of travelling waves.

This paper presents a detailed methodology to estimate VIV induced fatigue damage using time-domain rainflow counting algorithm for risers from NDP 2003 and Miami 2006 experiments. Dynamic strains and stresses are obtained from instantaneous riser displacements generated by the riser motion solver using a strain solver and a rainflow counting algorithm is employed to obtain stress cycles over the simulation period. Finally, Palmgren Miner's rule for the fatigue damage rate is applied to obtain effective fatigue damage over the riser.

2. Numerical formulation

2.1 Flow field solver

Finite-Analytic Navier-Stokes (FANS) approach is employed to solve the unsteady incompressible Navier-Stokes equation to simulate the flow field around the riser. The computational domain is discretized into smaller numerical elements. FANS method estimates a local-analytic solution of governing equation in the form of Fourier series and applies it to each numerical element locally. The system of equation thus formed is used to calculate the flow

variables for each nodal value. The continuity equation is solved using a finite volume approach and a hybrid PISO / SIMPLER algorithm is applied to update the pressure field around the riser. Large Eddy Simulation (LES) method is used to model the turbulence in the flow field where the high frequency turbulent fluctuations were filtered out using volume averaging. The filter width is taken as local grid size. The large vortices were simulated directly in LES and the smaller scale vortices are modeled using Smagorinsky's subgrid-scale turbulence model with the Smagorinsky's coefficient C_s taken as 0.1. A brief description of the LES method used in FANS algorithm can be found in Pontaza, Chen *et al*. (2005) and Huang, Chen *et al*. (2010).

2.2 Riser motion solver

Deepwater marine risers are generally modelled as tensioned beam with varying sectional properties along the riser. The riser motion solver uses an Euler-Bernoulli tensioned beam equation (Eq. (1)) with simply supported boundary conditions. The beam motion equation is linearized with variable tension and stiffness due to small transverse motions (a/D ~ 1) invoked by VIV in marine risers.

$$\begin{aligned} T\frac{d^2y}{dx^2}+\frac{dy}{dx}\frac{dT}{dx}-\frac{d^2}{dx^2}\left(EI\frac{d^2y}{dx^2}\right)+f_y &= m\ddot{y}+D_s\dot{y} \\ T\frac{d^2z}{dx^2}+\frac{dz}{dx}\frac{dT}{dx}-\frac{d^2}{dx^2}\left(EI\frac{d^2z}{dx^2}\right)+f_z &= m\ddot{z}+D_s\dot{z} \end{aligned} \tag{1}$$

where x is along the axial direction of the undistorted riser in calm water, while y and z denote the inline and crossflow directions, respectively, to the oncoming current. The material damping term D_s is neglected in the simulations presented in the paper. For horizontal riser as tested in NDP Experiments, the tension is kept constant ($dT/dx \approx 0$) in the simulation. The forces imposed by the fluid on the riser are represented by f_y and f_z which consist of the hydrodynamic forces generated by the FANS CFD algorithm. The beam equation is discretized using an implicit finite difference scheme which uses a direct integration approach at each time step. A zero motion boundary condition is applied at both ends of the riser to simulate the pinned condition and initial conditions are set to be zero based on the assumption that riser is stationary at the start of the simulation. Please refer to Huang, Chen *et al*. (2011) for more details.

2.3 Fatigue calculation module

The instantaneous displacements in inline $y(x,t)$ and crossflow $z(x,t)$ direction generated by riser motion solver is used to calculate instantaneous strain $\varepsilon(x,t)$ time series. The strain time series is related to the outer curvature of the riser at each time step (Eq. (2)). The dynamic stresses on the riser $\sigma(x,t)$ due to bending can be calculated as given in Eq. (3).

$$\varepsilon_{IL}=-\frac{D}{2}\frac{\partial^2 y}{\partial x^2}\Bigg/\left(1+\left(\frac{\partial y}{\partial x}\right)^2\right);\quad \varepsilon_{CF}=-\frac{D}{2}\frac{\partial^2 z}{\partial x^2}\Bigg/\left(1+\left(\frac{\partial z}{\partial x}\right)^2\right) \tag{2}$$

$$\sigma_{IL,CF}=E\varepsilon_{IL,CF} \tag{3}$$

The strain equation (Eq. (2)) is discretized using both a modal approach method and a finite difference discretization scheme. The modal method is used for NDP riser as the modes are well defined. This approach assumes the riser displacements as the summation of sinusoidal mode shapes (ξ). A least square method is employed to extract modal weight (w) and the instantaneous curvature can be obtained by double differentiation of the mode shapes. Another method using a direct finite difference scheme used to discretize Eq. (2) is utilized for riser from Miami 2006 experiments as the mode shapes for this vertical riser are not very well defined. The discretization scheme used is similar to Huang, *et al.* (2011). Similar method is used to determine both inline (y) and crossflow (z) direction strains and stresses.

Fatigue Damage D_f occurring in the risers is calculated using *rainflow counting algorithm* which is a time domain approach to calculate stress range cycles. This algorithm uses the stress time history $\sigma(x,t)$ as input and calculate stress ranges S_i and number of cycles n_i for which a particular stress range occurs. The stress range S_i is determined by calculating the peak and valley points (stress reversal points) in the stress time series and applying rainflow counting rules. A single slope S-N curve of the form given below (Eq. (4))

$$log_{10}(N_i) = log_{10}(a) - m\, log_{10}(S_i) \tag{4}$$

is used to calculate the maximum number of cycles to failure N_i. Miner's rule (Eq. (5)) is applied to calculate fatigue damage D_f over the length of time T from the summation of damage occurring from individual cycles n_i.

$$D_f = \frac{1}{T}\sum \frac{n_i}{N_i} \tag{5}$$

The fatigue damage rate thus obtained sheds light on the severity of VIV accumulated fatigue damage on deepwater marine risers. An illustration of fatigue damage algorithm calculation is presented in Fig. 1.

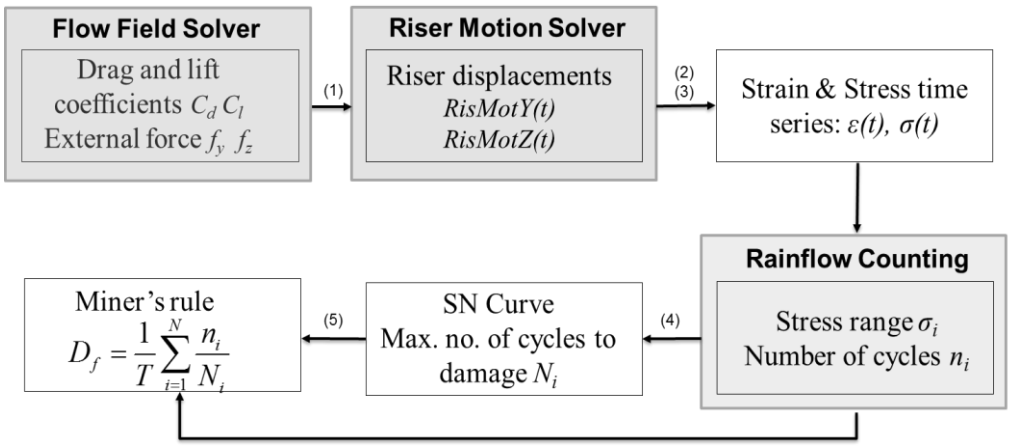

Fig. 1 Flowchart of the numerical approach

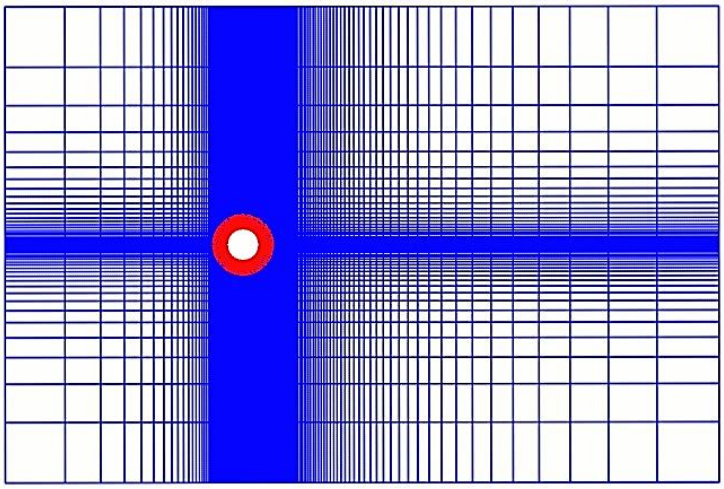

Fig. 2 Data grids at constant x/L

3. Results

3.1 Data grids

The grid system used in the VIV analysis using CFD is presented in Fig. 2 and the cross-sectional grid at constant axial location is shown. The curvilinear riser grid surrounds the riser is employed to calculate instantaneous riser displacements, vortex formation and provides interface for fluid structure interaction. Cartesian wake grid connects the riser grid to the background flow and is utilized to obtain enhanced resolution of vortex shedding. This overset (chimera) grid system assumes no relative movements between the grids and the grid location is updated at every iteration. The wake grid is kept sufficiently large to capture significant downstream vortices and to achieve negligible contribution of the lateral wall effects.

3.2 Horizontal riser in uniform currents

A horizontal riser with L/D ~ 1400 was used in experiments conducted by Norwegian Deepwater Programme (NDP) in 2003. The riser was towed using a crane to generate a uniform current profile. Bare and strake riser geometries were used and current profiles ranging U_{max} = 0.3 m/s – 2.4 m/s were simulated. In this section, four uniform current velocities are processed using the CFD approach for VIV calculations including 0.3 m/s, 0.7 m/s, 1.4 m/s and 1.7 m/s. The responses generated from CFD simulations are validated against the results published by Trim, Braaten *et al*. (2005) and Thorsen, Saevik *et al.* (2015). The simulation parameters are presented in Table 1.

Both crossflow and inline motion were studied for the above cases; however, inline motions did not reach a steady state of oscillations for higher current profiles. More number of iterations were required to process the inline motion which was not possible due to limited computer resources.

Fig. 3 presents the comparison of mean value of standard deviation from all the current velocities given in Table 1 with NDP experiments. The riser undergoes increasing sinusoidal

fluctuations at higher current velocities. Crossflow response is concentrated between 0.3 D – 0.6 D and the response envelope remains approximately the same for different velocities presented here.

As mentioned earlier, the riser vibrates at higher mode for high current speeds and high L/D ratios. In this paper, a least squares method is used for modal decomposition of the responses. This method assumes the displacements of a horizontally placed riser to be composed of sinusoids and their respective modal weights. The dominant mode corresponding to each current velocity using the method of least squares is presented in Fig. 4. Dominant mode is the mode where the maximum response spectrum is concentrated and has the maximum modal weight associated with it.

The number of modes acting on the system increases with increasing current velocity. At higher current velocities multiple modes act on the system which are function of the tension acting in the riser. For smaller velocities, a narrow band spectrum is observed with the peak frequency concentrated in a compact frequency range. A relatively broad band spectrum is observed in the case of higher current velocities as multiple frequencies act on the riser leading to a multi-mode response. The predicted peak frequency of the crossflow response and its comparison with the published results (Trim, Braaten *et al*. 2005) is shown in Fig. 5.

Table 1 CFD simulation parameters for uniform currents

Velocity	Riser Grid System	Wake Grid System	Reynolds Number	Dimensional time step (sec)
0.3 m/s	30 × 182 × 41	30 × 201 × 101	6.92×10^3	0.0009
0.7 m/s	30 × 182 × 41	30 × 201 × 101	1.16×10^4	0.000386
1.4 m/s	100 × 182 × 41	100 × 101 × 51	3.23×10^4	0.000193
1.7 m/s	100 × 182 × 41	100 × 101 × 51	3.92×10^4	0.000158

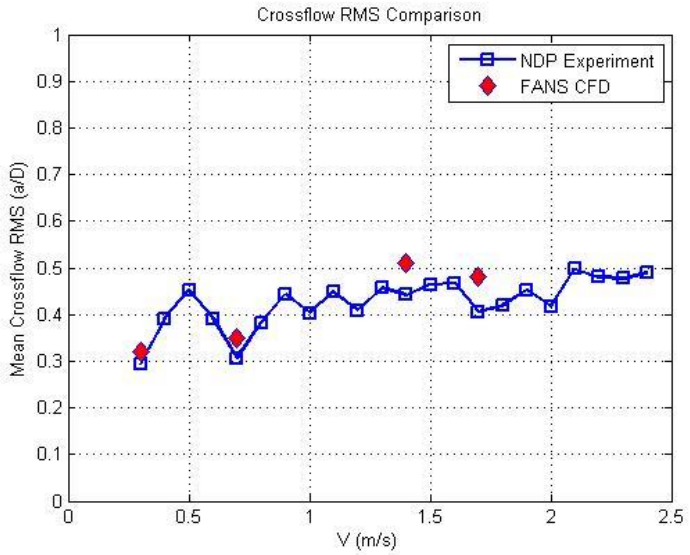

Fig. 3 Mean of crossflow motion standard deviation compared to NDP 2003 experiments

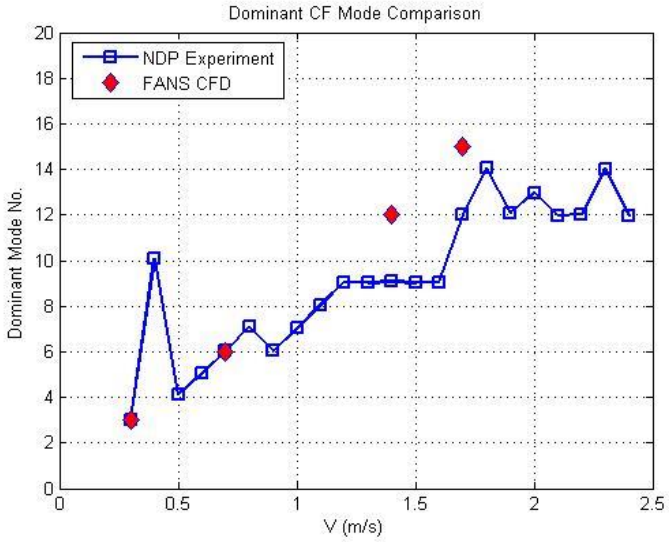

Fig. 4 Crossflow dominant mode comparison with NDP 2003 experiments

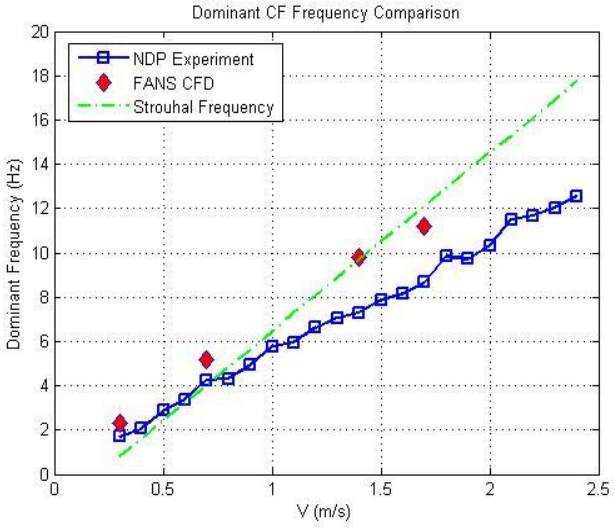

Fig. 5 Peak frequency of crossflow density spectrum compared to NDP 2003 experiments

Since the riser VIV response is tension dominated, the deviation of the experimental results and CFD simulation pertaining to the predicted dominant mode and peak frequency can be attributed to the tension variation in the range 4 kN-6 kN during experiments. In CFD simulation, the tension in the riser is assumed to be of a constant value of 5 kN. The fatigue predicted along the length of the riser for the four current velocities is shown in Fig. 6 and a comparison plot is presented in Fig. 7. A D curve (NORSOK standard, 1998) has been used for fatigue calculations. A conservative

fatigue prediction for lower current velocities is highly encouraging. The under-predicted fatigue damage at higher currents is a direct result of the inability of the simulations to reach fatigue convergence (Huang, Chen *et al*. 2008). Significantly more number of iterations are needed to reach the convergence limit which might improve predicted fatigue damage values. It is interesting to see that the riser fatigue response is not symmetrical along the riser. Even harmonics of riser fluctuations (i.e., dominant modes) lead to different amplitude of motion at the two ends of the riser which results in the unsymmetrical response.

3.3 Horizontal riser in sheared currents

To generate sheared current, the riser in NDP experiments was rotated using crane traversing a circular arc. This created a linearly sheared current profile with the end near the crane experiencing the maximum velocity. In this section, VIV analysis of two velocities are examined including U_{max} = 0.3 m/s and U_{max} = 0.7 m/s and both inline and crossflow damage has been studied. The properties of the aforementioned cases are given in Table 2.

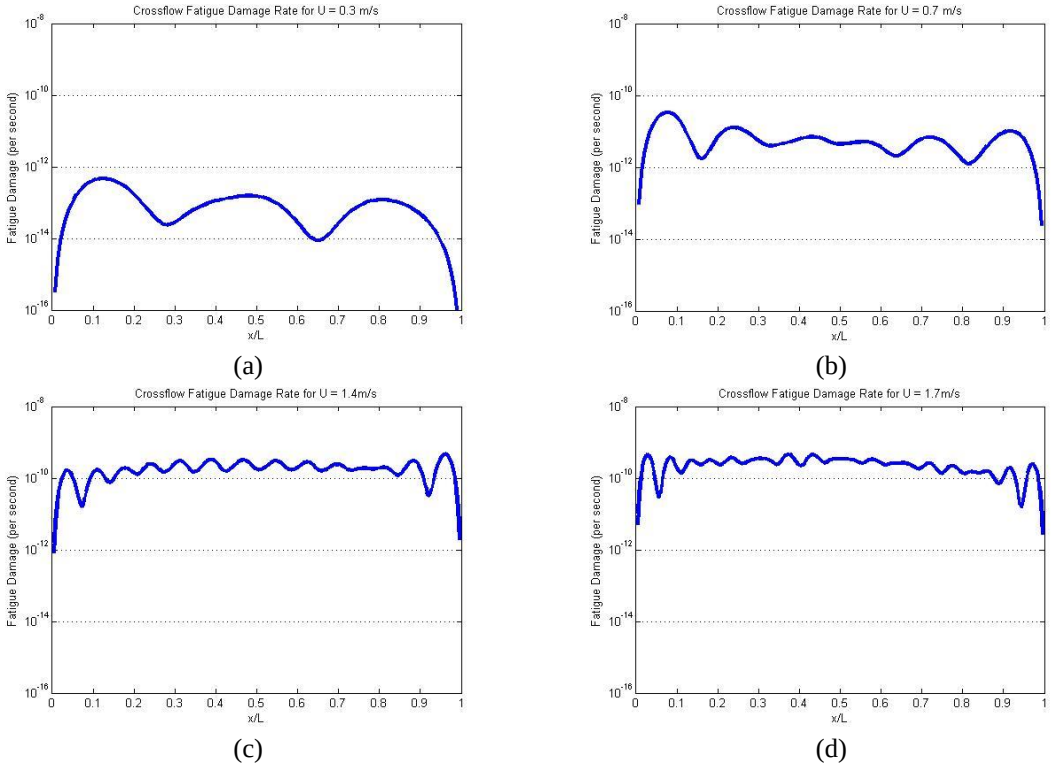

Fig. 6 Crossflow fatigue damage rate for (a) 0.3 m/s, (b) 0.7 m/s, (c) 1.4 m/s and (d) 1.7 m/s along the riser

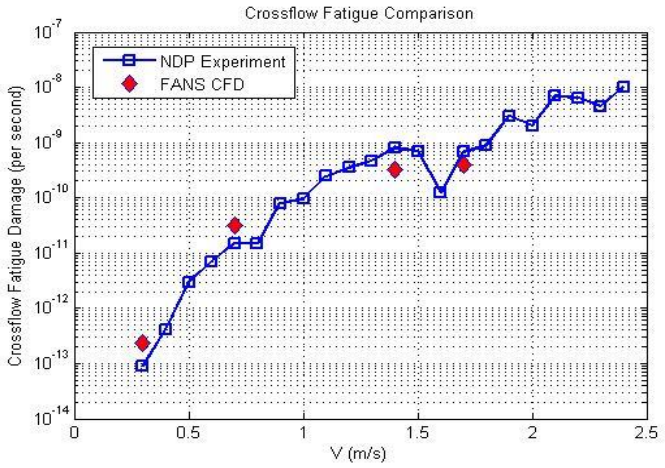

Fig. 7 Crossflow fatigue damage rate compared to NDP 2003 experiments

Table 2 CFD simulation parameters for linearly sheared currents

Velocity	Riser Grid System	Wake Grid System	Reynolds Number	Dimensional time step (sec)
0.3 m/s	30 × 182 × 41	30 × 201 × 101	6.92×10^3	0.0009
0.7 m/s	100 × 182 × 41	100 × 101 × 51	1.16×10^4	0.000386

Inline fatigue is generally ignored in commercial VIV analysis software as the inline motion is approximately less than 1/3rd of the crossflow motion. However, the inline frequency is twice of the crossflow frequency which causes more number of cycles in a given time period thereby affecting the fatigue damage rate. From the previous studies related to VIV fatigue damage on the riser, inline damage is shown comparable to crossflow damage (Trim, Braaten *et al*. 2005) and therefore it is essential for the VIV fatigue analysis codes to incorporate fatigue damage from both directions.

The riser crossflow and inline response for U_{max} = 0.3 m/s and U_{max} = 0.7 m/s is plotted in Figs. 8 and 9 along with mean and maximum value of the RMS response from the NDP experiments. For both crossflow and inline motion the mean and maximum values are seen to be in a reasonable comparison with the experiments.

The vortices generated downstream of the riser is presented in Fig. 10. Steady vortex street formation occurs relatively early in smaller current velocities and therefore as the current speed increases, more number of time steps are required for reaching steady state.

The modal decomposition of the response is shown in Figs. 11 and 12. 2nd and 4th mode are dominant in the crossflow and inline response of U_{max} = 0.3 m/s respectively, similar to the experiments. The dominant mode in crossflow and inline direction is 4th and 8th from the simulation and 5th and 10th from the experiments. One reason of this deviation could be the tension variations experienced during the NDP tests between 4 kN to 6 kN. The modes for vibration of the deepwater riser is extremely sensitive to tension and a slight variation of it could cause a different dominant mode response in the riser. For the CFD simulation the tension is assumed to be constant at 5 kN.

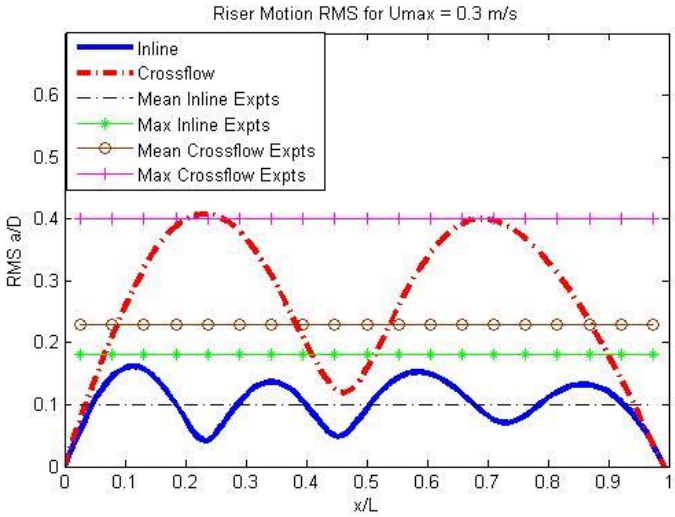

Fig. 8 RMS motion response for U_{max} = 0.3 m/s along the riser

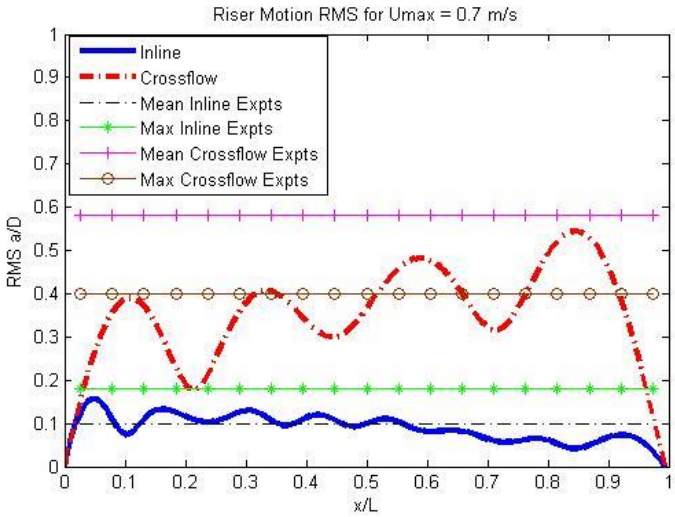

Fig. 9 RMS motion response for U_{max} = 0.3 m/s along the riser

The accumulated fatigue damage per year over the length of the riser is presented in Figs. 13 and 14. The SN Curve used for fatigue calculations is similar to the one used in uniform current analysis. The damage follows the trend similar to the RMS displacements along the riser. The maximum fatigue damage is reasonably predicted for 0.3 m/s, however, for 0.7 m/s the damage rate is over predicted in both inline and crossflow direction. Nevertheless, the damage prediction approach is conservative and both the inline and crossflow damage are shown to be comparable as expected from the NDP experiments.

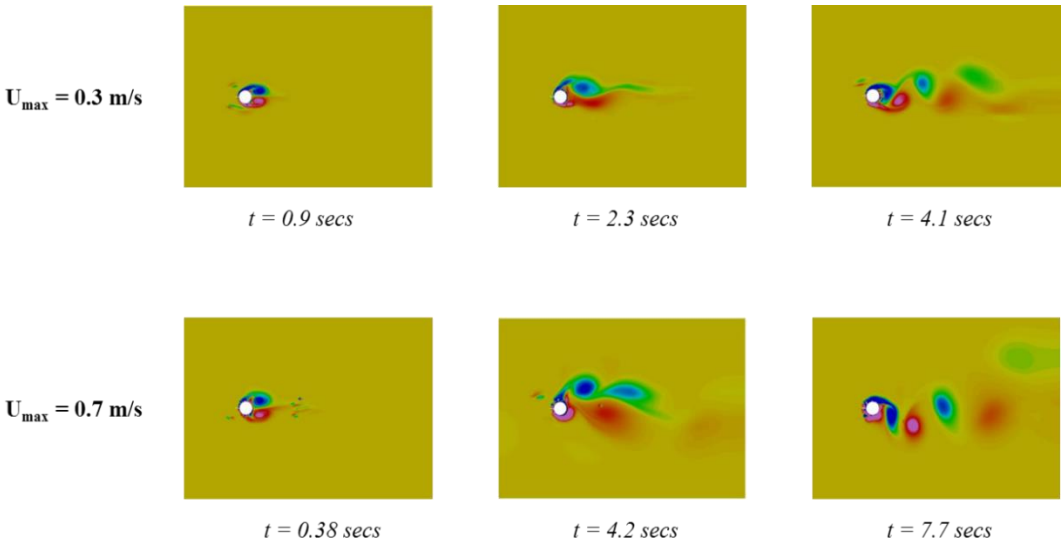

Fig. 10 Vortex evolution from aft of the riser for different time steps at x/L = 0.5

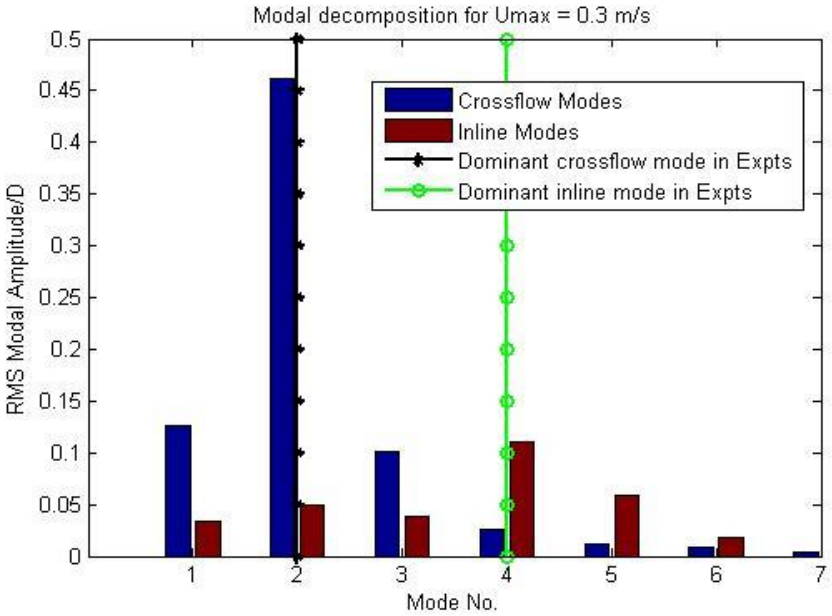

Fig. 11 RMS modal response for U_{max} = 0.3 m/s along the riser

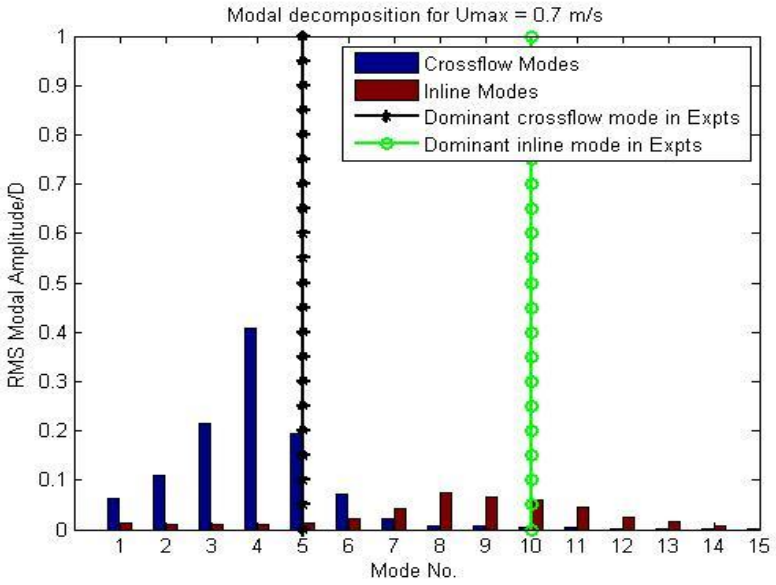

Fig. 12 RMS modal response for U_{max} = 0.7 m/s along the riser

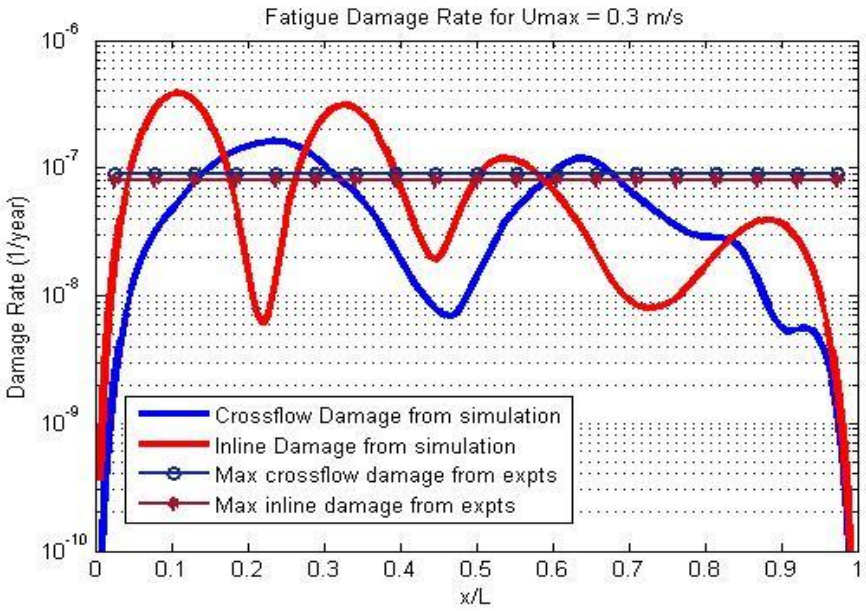

Fig. 13 Fatigue damage accumulation for U_{max} = 0.3 m/s along the riser

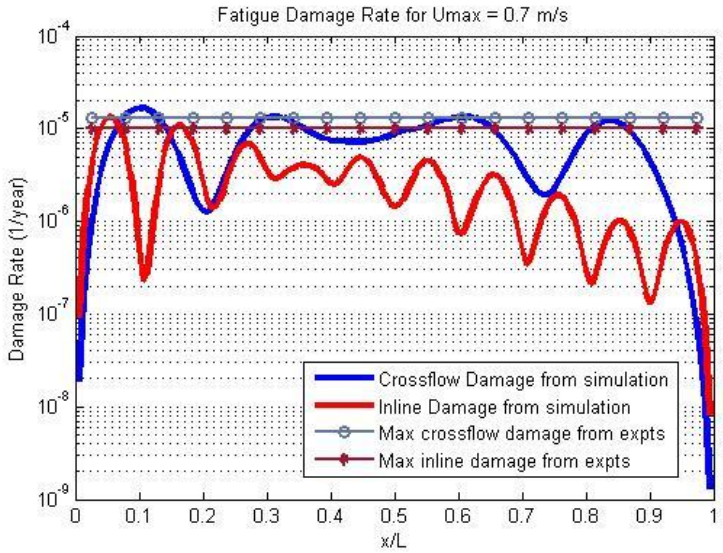

Fig. 14 Fatigue damage accumulation for U_{max} = 0.7 m/s along the riser

Occurrence of higher harmonics has been established by the NDP experiments as seen in Fig. 15. FANS CFD algorithm is able to predict the fundamental frequency response of the riser in sheared current reasonably but a finer axial grid resolution is needed to predict the response from higher harmonic (3x component). Thorsen, Saevik *et al.* (2015) stated that the higher harmonics have diminishing contributions towards fatigue damage as the sheared velocity is increased. Capturing higher harmonics is possible for low current velocities as the grid refinement studies require relatively lesser number of elements to fully capture the higher harmonics. For high currents, the fundamental frequency fatigue damage contributes a major portion of the total damage, 80% in some cases (Thorsen, Saevik *et al*. 2015), and with increasing computational capabilities it will be possible to achieve the contributions from the higher harmonics as well. Fatigue damage predicted by the CFD algorithm along with the damage from the fundamental frequency component and total crossflow damage from experiments is presented in Fig. 16.

3.4 Vertical riser in non –linearly sheared current

MIT and Deepstar (Vandiver, Jaiswal *et al*. 2006) conducted high mode number VIV experiments in the Gulf Stream with a composite pipe of L/D ~ 4200 in 2006. The riser was of length 152.5 m with an outer diameter of 3.6 cm and these characteristics were chosen so that high mode numbers can be simulated. The pipe was suspended from a research vessel and the bottom end of the pipe was attached to a railroad wheel to provide required tension. Since the pipe was vertically positioned a tension gradient was applied in the simulation with the bottom tension as 3225 N (weight of the railroad wheel) and the top tension as 3520 N (the weight of the railroad wheel added to the weight of the riser). The pipe was connected via universal joints such that a pinned boundary condition was created at both ends.

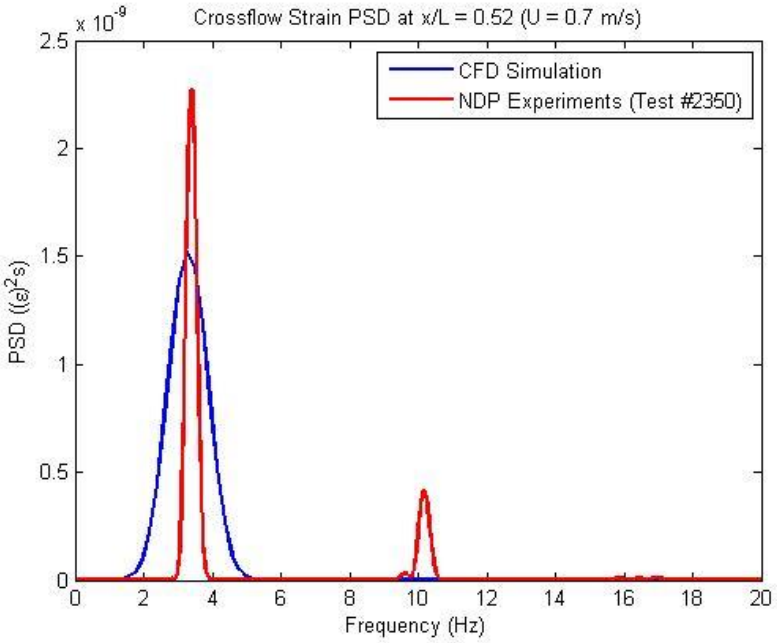

Fig. 15 Crossflow strain PSD comparison for U_{max} = 0.7 m/s

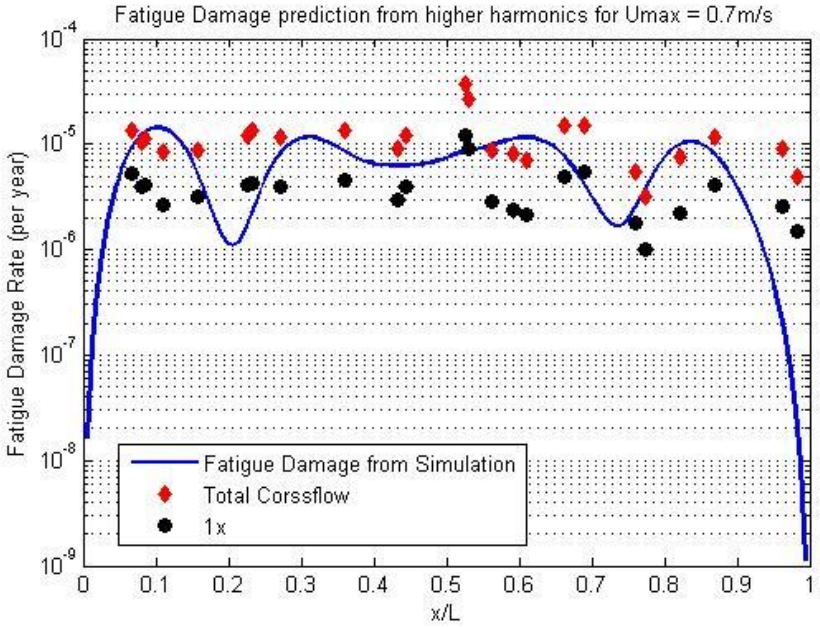

Fig. 16 Fatigue damage (incl. higher harmonics) compared to CFD simulation for U_{max} = 0.7 m/s

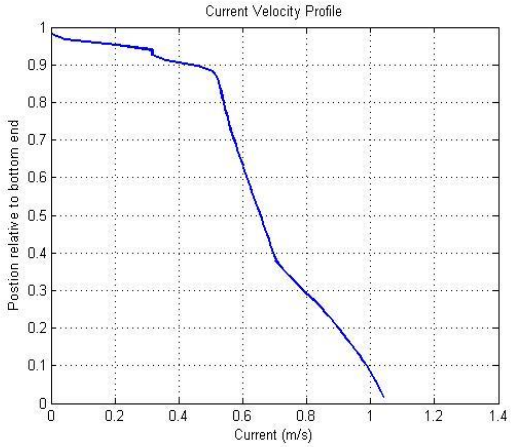

Fig. 17 Nonlinear sheared current for simulations

For the CFD simulation, a grid system with approximately 2.2 million elements is used and the simulation is run on a single node in a supercomputing facility. The riser grid has 150 × 182 × 41 elements and the wake grid consists of 150 × 141 × 51 elements.

A non-linearly sheared current velocity with U_{max} of ~1 m/s was experienced in the tests and has been applied to the simulation (Fig. 17). A dimensional time step of 0.0007 seconds was used with a Reynolds number of 3.37×10^4 and the simulation was run for 120000 time steps. The crossflow and inline displacement were obtained from the simulation. The riser was seen to displace about 300 D in inline direction before reaching steady state and only the steady state data for ~35 seconds is analyzed in this section and compared to the experimental results. The riser crossflow RMS is presented in Fig. 18 and the mean is observed to be 0.38 D which is typical in riser VIV analyses. Using a wavelet analysis, a steady state region of the experiments was derived and used for calculations.

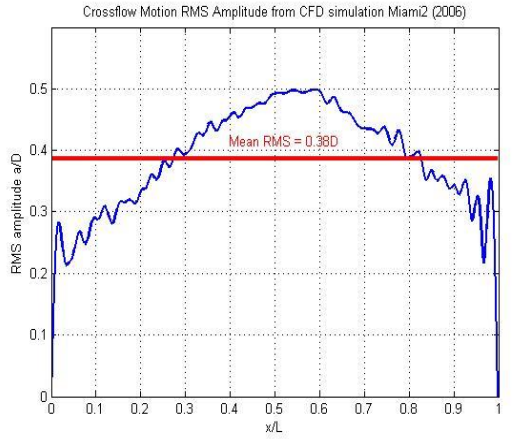

Fig. 18 Crossflow motion RMS along riser

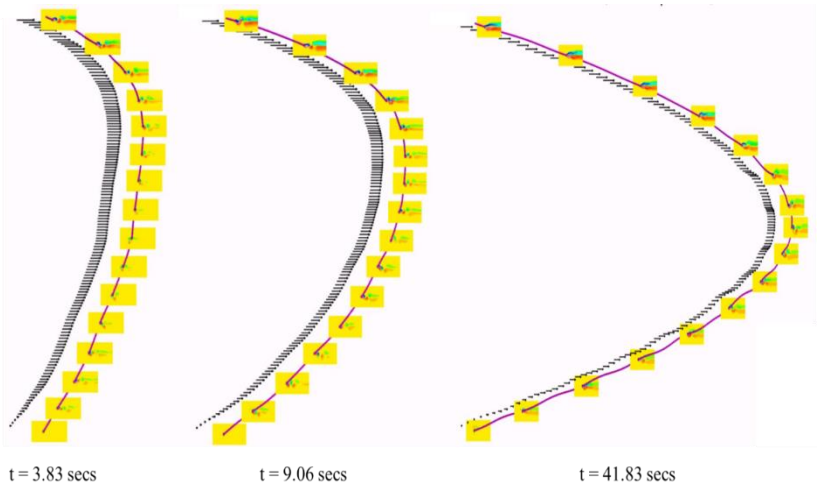

Fig. 19 Evolution of vortex shedding

The riser VIV evolution is presented in Fig. 19. The riser is initially stationary and it deflects in inline direction due to the fluid forces from the incoming currents. The tension provides the restoring force in the riser and the riser reaches equilibrium position when both the fluid forces and restoring forces balance which takes place after around ~30 seconds (~43000 iterations) in the simulation.

The riser crossflow bending strain (ε_{CF}) RMS comparisons are presented in Fig. 20 and can be seen in a very good agreement. The bending strain is higher as expected at the bottom end of the riser due to high incoming currents and low tension. The simulation results compare very well to the fundamental frequency component in the experiments.

The higher harmonics have not been predicted by the CFD solver as shown in Fig. 21. Results published by Huang, Chen *et al*. (2010) for a vertical riser with L/D ~ 482 had shown the occurrence of higher harmonics using similar CFD analysis approach. Near riser grid refinement and finer axial resolutions are needed to accurately predict higher harmonics for high Reynolds numbers and large L/D ratio. Moreover, the deviation of simulation results from the experiments can also be attributed to several issues which were encountered during the testing including the rotation of the inline and crossflow sensors. A method of instantaneous vector rotation was applied to achieve the true crossflow and inline strain signals. See Vandiver, Jaiswal *et al*. (2006). Other known problems with the experimental data such as current variability due to ship motions (heave, pitch and roll) and tension variations in the riser greatly affected the fatigue predicted from experiments as deepwater risers are tension dominated and very susceptible to oncoming currents. Nevertheless, the comparisons are very encouraging.

The fatigue damage rate predicted by the CFD simulation using rainflow counting algorithm shows similar trend to the bending strain RMS with highest damage occurring at x/L = 0.6– 0.9 as seen in Fig. 22. An API X' SN curve is used for fatigue calculations with a Young's Modulus of 200 GPa (Jhingran and Vandiver 2007). The fatigue damage from both 1x and total crossflow bending strain is presented and again the predicted fatigue damage from the simulations compares well with the 1st harmonic component from the experiments.

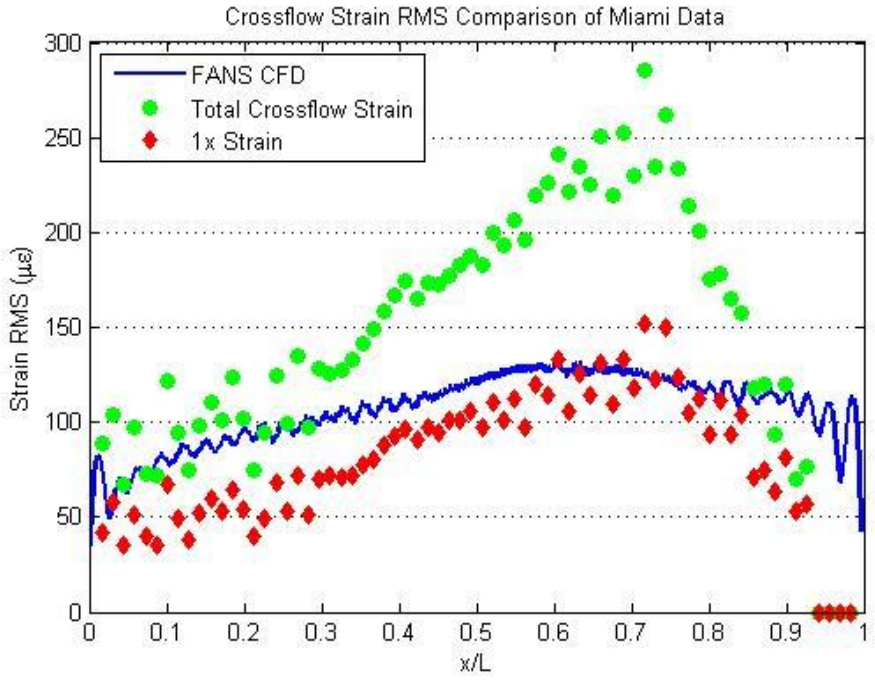

Fig. 20 Crossflow RMS strain comparisons between the CFD simulation and Miami experiments

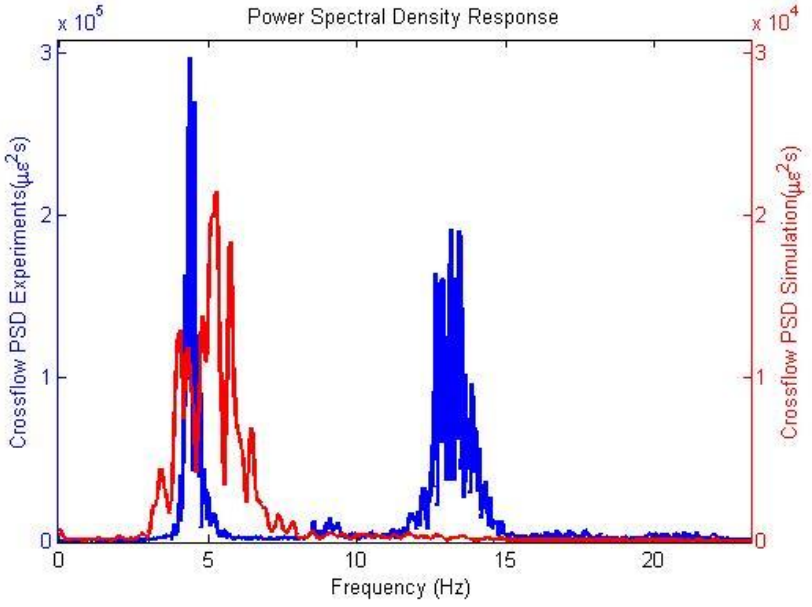

Fig. 21 Spectral density response of the strain time series from experiments and simulation

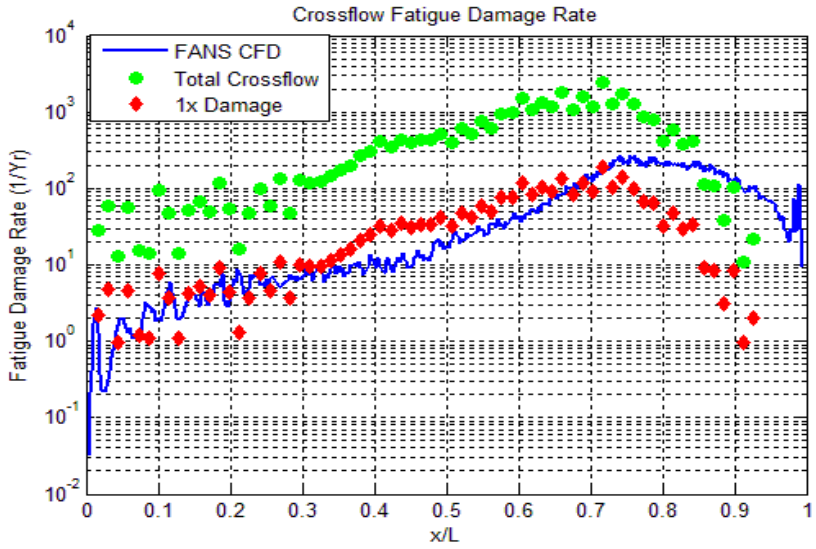

Fig. 22 Fatigue damage rate comparison between Miami experiments and CFD simulation

5. Conclusions

Riser VIV analyses presented in this paper are seen to be in a reasonable agreement with the experimental data and published results. Reynolds number up to 4×10^4 studied in the paper portray a realistic representation of the marine environment. The finite-analytic scheme with a tensioned beam motion solver and rainflow counting module are benchmarked with comparisons from experiments and the overall fatigue damage is reasonably predicted by the fatigue module. Lower current speeds and smaller L/D values are in perfect agreement with the field data; however, more complex current profiles and high L/D ratios are more difficult to resolve. At high L/D ratios the riser is influenced greatly by the complexities of the incoming flow field. Nevertheless, with increasing computational efficiency and optimal parallel processing algorithms, the flow physics associated with these complexities can be resolved with significant accuracy using the FANS CFD solver and fatigue module developed in this paper.

Grid convergence studies were performed for lower current velocities and the statistics presented varied little with further grid resolutions. For the higher current velocities with U_{max} = 1 – 1.7 m/s, a grid convergence study proved to be very expensive and time intensive. Multiple dominant modes were observed for higher current speeds and are seen to be strongly dependent on the tension in the risers. The tension was seen to be varying in both NDP (2003) and Miami (2006) experiments whereas the tension was assumed constant in the simulations which led to the difference in dominant modes and peak frequencies predicted by simulation and tests. The crossflow RMS for all the cases stayed within 0.4 D – 0.6 D which is typical of the VIV experienced by deepwater risers. The inline motion amplitude was approximately 1/3rd of the crossflow motion amplitude with the peak frequency occurring at twice the crossflow frequency. The fatigue damage values followed the trends similar to the motion RMS and the inline damage was shown comparable to the crossflow damage. The fatigue damage prediction algorithm using

CFD presented extremely encouraging results including cases with highly sheared and extremely long risers.

References

Bearman, P.W. (1984), "Vortex shedding from oscillating bluff bodies", *J. Fluid Mech.*, **16**, 195-222.

Blevins, R.D. (1990), *Flow-Induced Vibrations*, (2nd Edition), Van Nostrand Reinhold, New York, USA.

Constantinides, Y. and Oakley, O.H. (2008), "Numerical prediction of VIV and comparison with field experiments", *Proceedings of the ASME 27th International Conference on Offshore Mechanics and Arctic Engineering*, Estoril, Portugal, June.

Holmes, S., Oakley, O.H. and Constantinides, Y. (2006), "Simulation of Riser VIV Using Fully Three Dimensional CFD Simulations", *Proceedings of the 25th International Conference on Offshore Mechanics and Arctic Engineering*, Hamburg, Germany, June.

Huang, K., Chen, H.C. and Chen, C.R. (2007), "Riser VIV analysis by a CFD approach", *Proceedings of the 17th International Offshore and Polar Engineering Conference*, Lisbon, Portugal, July.

Huang, K., Chen, H.C. and Chen, C.R. (2008), "Riser VIV induced fatigue assessment by a CFD approach", *Proceedings of the 18th International Offshore and Polar Engineering Conference*, Vancouver, Canada, July.

Huang, K., Chen, H.C. and Chen, C.R. (2010), "Vertical riser VIV simulation in uniform current", *J. Offshore Mech. Arct*., **132** (3), 1-10.

Huang, K., Chen, H.C. and Chen, C.R. (2011), "Numerical scheme for riser motion calculation during 3-D VIV simulation", *J. Fluid. Struct.*, **27**(7), 947-961.

Huang, K., Chen, H.C. and Chen, C.R. (2012), "Vertical riser VIV simulation in sheared current", *Int. J. Offshore Polar*, **22**(2), 142-149

Jhingran, V. and Vandiver, J.K. (2007), "Incorporating the higher harmonics in VIV fatigue predictions", *Proceedings of the 26th International Conference on Offshore Mechanics and Arctic Engineering*, San Diego, USA, June.

Lie, H. and Kaasen, K.E. (2006), "Modal analysis of measurements from a large-scale VIV model test of a riser in linearly sheared flow", *J. Fluid. Struct.*, **22**(4), 557-575.

Lucor, D., Mukundan, H. and Triantafyllou, M.S. (2006), "Riser modal identification in CFD and full-scale experiments", *J. Fluid. Struct.*, **22**(6-7), 905-917.

Meneghini, J.R., Saltara, F., Fregonesi, R.A., Yamamoto, C.T., Casaprima, E. and Ferrari, J.A. (2004), "Numerical simulations of VIV on long flexible cylinders immersed in complex flow fields", *Eur. J. Mech. B/Fluid.*, **23**(1), 51-63.

Mukundan, H., Modarres-Sadeghi, Y., Dahl, J.M., Hover, F.S. and Triantafyllou, M.S. (2009), "Monitoring VIV fatigue damage on marine risers", *J. Fluid. Struct.*, **25**(4), 617-628.

Newman, D.J. and Karniadakis, G.E. (1997), "A direct numerical simulation study of flow past a freely vibrating cable", *J. Fluid Mech*., **344**, 95-136

Pontaza, J.P., Chen, C.R. and Chen, H.C. (2004), "Chimera Reynolds averaged Navier-Stokes simulations of vortex-induced vibration of circular cylinders", *Proceedings of the International ASCE Conference: Civil Engineering in the Oceans VI*, 166-176.

Pontaza, J.P., Chen, C.R. and Chen, H.C. (2005a), "Simulations of high Reynolds number flow past arrays of circular cylinders undergoing vortex-induced vibrations", *Proceedings of the 15th International Offshore and Polar Engineering Conference*, Seoul, Korea, June.

Pontaza, J.P., Chen, H.C. and Chen, C.R. (2005b), "Numerical simulations of riser vortex-induced vibrations", *Proceedings of the 2005 Society of Marine Engineers and Naval Architects (SNAME) Conference*, **52**, 1-12.

Pontaza, J.P., Chen, H.C. and Reddy, J.N. (2005), "A local-analytic-based discretization procedure for the numerical solution of incompressible flows", *Int. J. Numer. Meth. Fl*., **49**, 657-699.

Pontaza, J.P. and Chen, H.C. (2007), "Three-dimensional numerical simulations of circular cylinders undergoing two degree-of-freedom vortex-induced vibrations", *J. Offshore Mech. Arct.*, **129**(3), 158-164.

Thorsen, M.J., Saevik, S. and Larsen, C.M. (2015), "Fatigue damage from time domain simulation of combined in-line and cross-flow vortex-induced vibrations", *Marine Struct.*, **41**, 200-222.

Tognarelli, M.A., Taggart, S. and Campbell, M. (2008), "Actual VIV Fatigue Response of Full Scale Drilling Risers: With and Without Suppression Devices", *Proceedings of the ASME 27th International Conference on Offshore Mechanics and Arctic Engineering* (OMAE), Estoril, Portugal, June.

Trim, A.D., Braaten, H., Lie, H. and Tognarelli, M.A. (2005), "Experimental investigation of vortex-induced vibration of long marine risers", *J. Fluid. Struct.*, **21**, 335-361.

Vandiver, J.K., Jaiswal, V., Swithenbank, S.B. and Jhingran, V. (2006), "Fatigue damage from high mode number vortex-induced vibration", *Proceedings of the 25th International Conference on Offshore Mechanics and Arctic Engineering*, Hamburg, Germany, June.

MK